Am J Cancer Res 2023;13(6):2323-2341
www.ajcr.us /ISSN:2156-6976/ajcr0143948

Original Article

USP37 promotes angiogenesis and metastasis in colorectal cancer by facilitating β-catenin stability

Dafeng Tong[1*], Jie Yuan[1,2*], Zhaoming Wang[1*], Enda Yu[1], Jifu E[1]

[1]*Department of Colorectal Surgery, Changhai Hospital, Navy Military Medical University, Shanghai, China;* [2]*Department of Rehabilitation, Beidaihe Rehabilitation and Recuperation Center for PLA Joint Logistics Support Force, Qinhuangdao, Hebei, China.* [*]*Co-first authors.*

Received May 6, 2022; Accepted March 9, 2023; Epub June 15, 2023; Published June 30, 2023

Abstract: Ubiquitin-specific peptidase 37 (USP37) is a novel deubiquitinating enzyme, which has been found to be involved in the progression of multiple tumors. However, its function in colorectal cancer (CRC) remains unclear. Here, we firstly proved that USP37 was up-regulated in CRC cases, and high USP37 expression predicted poor survival of CRC cases. USP37 up-regulation promoted the proliferation, cell cycle progression, apoptosis inhibition, migration, invasion, epithelial mesenchymal transition (EMT) and stemness of CRC cells; moreover, USP37 facilitated the angiogenesis of human umbilical vein endothelial cells (HUVECs). However, USP37 silencing showed the opposite function. *In vivo* experiment suggested that USP37 silencing suppressed the growth and lung metastasis of CRC in nude mice. Interestingly, we found that CTNNB1 (gene coding for β-catenin) level was positively correlated with USP37 level in CRC and USP37 silencing suppressed the expression of β-catenin in CRC cells and xenograft tumor tissues. Further mechanistic studies showed that USP37 could enhance the stability of β-catenin by inhibiting its ubiquitination. Taken together, USP37 acts as an oncogene in CRC, which promotes angiogenesis, metastasis and stemness by enhancing β-catenin stability via inhibiting its ubiquitination. USP37 may be a usefully target in CRC clinical treatment.

Keywords: CRC, USP37, angiogenesis, metastasis, β-catenin stability

Introduction

Colorectal cancer (CRC) is the world's third-most-common cancer and the second leading cause of cancer-related death, accounting for 8%-9% of all cancer patients [1, 2]. Every year, more than 945,000 people worldwide are diagnosed with CRC and over 492,000 patients die from it. Even worse, up to 20% of CRC patients develop metastases, with lung and liver metastases being the most common [3]. Environmental factors, lousy eating habits, and genetic factors all have a role in CRC etiology [4]. Early surgical resection can enhance the 5-year survival rate, whereas patients with advanced CRC have a very poor diagnosis [5]. In most CRC patients, recurrence and metastasis are the leading causes of death [6]. Surgical resection and chemotherapy are two of the most common treatments for CRC. However, these treatment strategies do not significantly improve the prognosis of CRC patients, particularly those with recurrence or metastasis. Simultaneously, the adverse side effects and high financial expenditures have significantly impacted the quality of life of CRC patients and brought a severe economic burden to the family [7]. Therefore, understanding the molecular mechanisms of the pathogenesis and progression of CRC will help discover effective therapeutic targets for CRC to improve the prognosis of CRC patients.

Ubiquitin-specific peptidase 37 (USP37) is a novel deubiquitinating enzyme that belongs to the ubiquitin-specific processing protease family and Ubiquitin-specific peptidase 37 (USP37) is a novel deubiquitinating enzyme that belongs to the ubiquitin-specific processing protease family and has 979 amino acids [8, 9]. The function of USP37 is identified as a potent cell cycle regulator, and its overexpression can speed up the transition from G1 to S phase of the cell cycle [10, 11]. Recent studies have found that

USP37 promotes tumor growth in in multiple cancers [12, 13]. One of the significant oncogenic drivers of clear cell renal cell carcinoma is Hypoxia-inducible factor 2α (HIF2α). Intriguingly, USP37 can improve the stability of HIF2α protein by promoting its deubiquitination, thereby promoting primary renal tumorigenesis and lung metastasis [14]. USP37 expression is associated with higher mortality and positively correlated with breast cancer metastasis. It is considered a key target for the clinical treatment of breast cancer, as USP37 up-regulation can intensify the stemness, invasiveness, and epithelial-mesenchymal transition (EMT) of breast cancer cells [15]. Moreover, by inhibiting Snail1 protein degradation, USP37 can intensify the proliferation and migration of gastric and lung cancer cells. USP37 is thus considered a potential therapeutic target to limit the metastasis of gastric and lung cancers [16, 17].

However, However, until now, no literature has been published on the exact function and involvement of USP37 in CRC development. We analyzed the expression of USP37 in CRC patients by using the Cancer Genome Atlas (TCGA) database. USP37 was discovered to be aberrantly up-regulated in CRC tissues compared to neighboring normal tissues. Thus, we speculated that USP37 might play a tumor-promoting role in CRC. This study used various *in vitro* and *in vivo* experiments to validate this speculation. β-catenin is a protein encoded by the proto-oncogene CTNNB1, which is overexpressed in CRC and aggravates the EMT and metastasis of CRC cells [18, 19]. In our preliminary TCGA analysis, we discovered that the level of CTNNB1 was positively linked with the USP37 level in CRC tissues. The study verified whether USP37 promoted CRC development via mediating the stability of the β-catenin protein. This is the first time that the specific function and mechanism of USP37 in regulating CRC has been clarified and has significant clinical implications.

Methods

TCGA analysis

We downloaded the clinical expression profiles of USP37 in COAD cases from the TCGA database, including USP37 expression data in 290 tumor tissues and 349 adjacent normal tissues from the GTEx-COAD profile, USP37 expression data in 480 tumor tissues and 41 adjacent normal tissues from TCGA-COAD profile, and USP37 expression data in 41 paired tumor tissues and adjacent normal tissues from TCGA-COAD profile. The R programming language was used to examine the USP37 expression data. We also used Spearman correlation analysis to analyze the correlation between USP37 and CTNNB1 (coding β-catenin protein) expression based on the TCGA-COAD and TCGA-READ profiles.

Patients' enrollment and clinical tissues

Tumor tissues and the paired adjacent normal tissues were harvested from 106 CRC cases. All the 106 CRC cases were enrolled at Changhai Hospital between April 2015 and November 2016. Experienced pathologists confirmed that all of these instances were CRC, and none had anti-cancer medication before surgery. The clinical tissues were stored in liquid nitrogen after being resected during surgery. These cases were monitored for 2000 days after surgery, with death as the endpoint. The 2000-day overall survival of these CRC cases was evaluated by the Kaplan-Meier survival curve.

Every case has signed a written informed consent form. This study has been ratified by the Ethics Committee of Changhai Hospital.

Cell lines and transfection

Normal human intestinal epithelial cell line (NCM460) and CRC cell lines (HCT116, SW620, LoVo, SW480, and T84) were all commercially provided by the American Type Culture Collection (ATCC, Manassas, VA, USA). Each cell line was independently grown into Dulbecco's modified Eagle's medium (DMEM, Zeye Biotechnology, Shanghai, China) suspended with 10% fetal bovine serum (FBS, Beyotime, Shanghai, China) at 37°C, 5% CO_2.

HCT116 and T84 cells were separately transfected with USP37 expression vectors, empty vectors, shRNA (#1 and #2) targeting USP37 and scramble (GeneChem, Shanghai, China) to regulate USP37 expression. HCT116 and T84 cells were harvested at about 85% confluence and suspended in non-serum DMEM cell suspension (1×10^6 cell/mL). A total of 1 mL of the cell suspension was collected and cultivated

into 6-well plates. The transfection was then implemented using Lipofectamine 3000 (Thermo Fisher Scientific, Shanghai, China) as directed by the manufacturer. After transfection, cells were cultured for 48 h with DMEM with 10% FBS at 37°C and 5% CO_2. Western blot was used to determine the effectiveness of the transfection.

Tetrazolium dye (MTT) assay

HCT116 and T84 cells were collected and then dispersed in DMEM (with 10% FBS) to make a cell suspension (1×10^5 cell/mL). The cell suspension with a volume of 100 μL was collected and cultivated into 96-well plates at 37°C, with 5% CO_2. The cells were cultured for 48 h before being treated for 4 h with MTT solution (5 mg/mL, 10 L). After that, dimethyl sulfoxide was added with 150 μL per well, and the plates were shaken for 10 min to dissolve the crystals fully. The plates were placed on a multi-well microplate reader (Molecular Devices, Shanghai, China) for the absorbance value measurement at 450 nm.

Flow cytometry

Cell cycle distribution of HCT116 and T84 cells was analyzed by flow cytometry. HCT116 and T84 cells were separated with 0.25% trypsin and washed in pre-cooled phosphate-buffered saline (PBS). The cells were then fixed overnight in a -20°C refrigerator using pre-cooled ethyl alcohol (70%). The cells were then rinsed in PBS and stained with propidium iodide (PI) for 15 min in the dark. The cell cycle distribution analysis was performed using a flow cytometer (Beckman Coulter, Brea, CA, USA). Additionally, the apoptosis of HCT116 and T84 cells was assessed using the Annexin V-FITC /PI kit (Zeye Biotechnology, Shanghai, China) in line with the kit directions. Flow cytometry was used to determine the apoptosis percentage.

Wound healing assay

HCT116 and T84 cells were cultured with DMEM (with 10% FBS) in 6-well plates with 1×10^6 cells/mL per well. A micropipette tip was used to produce a wound in the bottom of the plates after the cells had grown adherently. The floating cells and debris were removed by washing the cell twice with PBS. The cells were then cultured with 1 mL fresh DMEM (without FBS) for 24 h at 37°C, with 5% CO_2. The initial (0 h) and the final (24 h) wound width were recorded to calculate the relative wound width with the formula of the final (24 h) wound width/the initial (0 h) wound width.

Transwell experiment

The invasion potential of HCT116 and T84 cells was determined using transwell chambers. Matrigel (Beyotime, Shanghai, China) was diluted in serum-free DMEM eight times before being applied to the upper chambers. A total of 5×10^5 cells were suspended into 1 mL of the serum-free DMEM, and 200 μL was collected and inoculated into the upper chambers. We filled the lower compartments with 600 μL of DMEM (with 10% FBS). The cells were induced for 24 h at 37°C, with 5% CO_2. The invasive adhered to the lower surface of the chambers were fixed with 4% paraformaldehyde for 10 min and stained with 0.1% cresyl violet for 10 min. The invasion HCT116 and T84 cells were photographed and counted in five non-overlapping fields of view under a microscope (Olympus, Tokyo, Japan).

Moreover, the Transwell experiment was used to assess the migration ability of human umbilical vein endothelial cells (HUVECs, ATCC, Manassas, VA, USA). To suspend HUVECs, we collected the culture medium of HCT116 and T84 cells in each group. In brief, HCT116 and T84 cells of each group were cultured for 48 h 37°C, with 5% CO_2. The culture medium was then collected and used to suspend HUVECs. The Transwell chambers (without Matrigel) were employed for the migration detection, as stated above.

Sphere-forming assay

HCT116 and T84 cells of each group were inoculated into 6-well ultralow attachment plates (1×10^3 cells per well), and cultured with DMEM (without serum) containing FGF (10 ng/mL), EGF (10 ng/mL), penicillin (100 units/mL) and streptomycin (100 μg/mL) for 14 days. The culture medium was refreshed at a 3-day interval. After 14 days, the sphere formation was observed under a microscope (Olympus, Tokyo, Japan).

Angiogenesis assay

The angiogenesis assay was used to examine the effect of USP37 on angiogenesis. The

24-well plates were pre-coated with 50 μL Matrigel (Beyotime, Shanghai, China). To collect the culture media, HCT116 and T84 cells were cultured for 48 h. The HUVECs were then cultured with 200 μL of the above culture medium for 12 h (at 37°C, 5% CO_2) with 2×10^4 cells per well. The tube formation was then observed under a microscope (Olympus, Tokyo, Japan).

Enzyme-linked immunosorbent assay (ELISA) assay

The culture medium of HUVEC cells was collected after 48 h of culture. The supernatant of the culture medium was collected after centrifugation and used to determine the level of vascular endothelial growth factor A (VEGFA) using an ELISA kit (Solarbio, Beijing, China). The detection procedure was implemented in line with the kit directions.

In vivo growth and lung metastasis experiments

The animal study has been approved by the Animal Ethics Committee of Changhai Hospital. Cavens Laboratory Animal Co., Ltd. (Changzhou, Jiangsu, China) provided us with twenty-four BALB/c nude mice (5 weeks old, 220-230 g in weight). Mice were kept in a specific-pathogen-free room at (22 ± 2)°C with a 12 h day/night cycle. There was plenty of food and water to go around.

HCT116 cells were collected and suspended in PBS after being treated with a scramble and USP37 shRNA (#2). The cell suspension had a density of 1×10^7 cells/mL. The xenograft model was created by subcutaneous injection of 100 μL of the cell suspension into the right abdominal cavity of mice. Each cell suspension sample was injected with six mice. The length and width of the xenograft tumor were measured every seven days to estimate the xenograft tumor volume by (length × width^2)/2. Mice were sedated with 5% isoflurane on day 28 after injection, and euthanized by rapid cervical dislocation. Before being weighted, the xenograft tumor was removed and then washed in PBS. The xenograft tumor was maintained in a refrigerator at -20°C after weighing it.

For *in vivo* lung metastasis assay, each suspension (100 μL) of HCT116 cells was injected into the tail vein of six mice. The trial was ended four weeks later. The lungs were collected after mice were euthanized and were stored in a refrigerator at -20°C.

Immunohistochemistry (IHC)

The xenograft tumor and clinical tissues were fixed in 10% formalin for 24 h before being embedded in paraffin. After being cut into 4 μm tissue slices, the sections were dewaxed and rehydrated using a combination of xylene and graded alcoholt. After removing endogenous peroxidase activity (by 3% H_2O_2 treatment) and the antigen retrieval (by citrate buffer treatment), the sections were blocked by 5% normal goat serum for 20 min at room temperature. USP37 (1:100, ab229092, Abcam, Shanghai, China), Ki67 (1:100, ab1558, Abcam, Shanghai, China) and β-catenin (1:100, ab16051, Abcam, Shanghai, China) primary antibodies were recruited respectively for the immunostaining of the sections for 12 h at 4°C. The sections were then treated with a biotin-labeled secondary antibody working solution (1:200, Yeasen Biological Technology, Shanghai, China) for 30 min at 37°C. The sections were thoroughly rinsed with tap water after being stained by 3,3-diaminobenzidine (DAB) and counterstained by hematoxylin. Separately executing graded alcohol treatment and xylene treatment, dehydration and transparency were implemented progressively. After being sealed, the sections were observed under a microscope (Olympus, Tokyo, Japan).

Hematoxylin and eosin (H&E) staining

The lungs of mice were fixed by 10% formalin, embedded in paraffin, dewaxed with xylene, rehydrated with graded alcohol, and then cut into 4 μm pieces. Hematoxylin solution was used to stain the sections for 5 min, then 1% hydrochloric acid alcohol was used to distinguish them for a few seconds, and then 0.6% ammonia water was used to color them blue. Eosin solution was then used to counterstain sections for 2 min. After being dehydrated (by graded alcohol treatment) and transparent (by xylene treatment), the sections were sealed to observe the nodules under a microscope (Olympus, Tokyo, Japan).

Quantitative real-time polymerase chain reaction (qRT-PCR)

qRT-PCR was used to measure the expression of USP37 mRNA in tissues. Briefly, the entire

lysates of tissues were collected using the Trizol reagent. The supernatant was then harvested by centrifugation, and the concentration of total RNA in the supernatant was measured. Using the Reverse Transcription Kit (TaKaRa, Dalian, China), 2 μg of the supernatant was collected, and reverse transcription. The reverse transcription was implemented in line with the kit directions. qRT-PCR was subsequently executed by recruiting the SYBR Premix EX Tag Master mixture kit (TaKaRa, Dalian, China) and the iCycler™ Real-Time System (Bio-Rad Laboratories, Richmond, CA, USA). This procedure was followed exactly as directed by the manufacturer. The procedure was 95°C for 15 s, then 40 cycles of 95°C for 5 s and 60°C for 30 s. The primers were as follows: USP37 sense 5'-GGCAGCAAGTCATCATTCCA-3' and antisense 5'-GGCTGGTGATGCAGGAATTC-3'; β-actin sense 5'-CATGTACGTTGCTATCCAGGC-3' and antisense 5'-CTCCTTAATGTCACGCACGAT-3'. β-actin was used as the reference. The relative USP37 mRNA expression was calculated by the $2^{-\Delta\Delta Ct}$ method.

Co-immunoprecipitation assay

Co-immunoprecipitation assay on 293T cells were used to investigate the interaction between USP37 and β-catenin proteins. ATCC (Manassas, VA, USA) provided the 293T cells used in this investigation. In short, 1×10^5 293T cells were grown into 6-well plates with 1 mL DMEM (without 10% FBS). The cells were then transfected with HA-USP37 and Flag-β-catenin vectors (GeneChem, Shanghai, China) alone or in combination. Cells were collected after being grown for 48 h at 37°C, with 5% CO_2. To obtain the whole lysates, cells were treated with radio-immunoprecipitation assay (RIPA) lysis buffer (Beyotime, Shanghai, China). Then the supernatant of the whole lysates was collected by centrifugation. The supernatant with a volume of 50 μL was used as the input. By incubating an equal amount of the supernatant with anti-FLAG and anti-HA beads, co-immunoprecipitation was achieved (Beyotime, Shanghai, China). Western blot was used to confirm the co-immunoprecipitated proteins.

MG132 and CHX treatment

This study used MG132 (10 μM) and cycloheximide (CHX, 10 μM) to treat HCT116 and T84 cells to investigate h the underlying mechanism of USP37 regulating β-catenin expression. HCT116 and T84 cells (1×10^6 cells) were cultivated with 1 mL DMEM (with 10% FBS) containing MG132 (10 μM) in 6-well plates for 8 h at 37°C, with 5% CO_2. In addition, DMEM (with 10% FBS) with 10 μM CHX was given to treat HCT116 and T84 cells for 4, 8, and 12 h at 37°C, with 5% CO_2. HCT116 and T84 cells were collected at the indicated time points to discover the expression of USP37 and β-catenin proteins using Western blot.

Ubiquitination assay

To research whether USP37 facilitates β-catenin protein stability by deubiquitination, this study collected HCT116 and T84 cells treated by MG132, by USP37 shRNA, and co-treated by MG132 and USP37 shRNA for ubiquitination assay. HCT116 and T84 cells without any treatment were served as control. After harvested, HCT116 and T84 cells were lysed by RIPA lysis buffer for 1 h at 4°C for the collection of total proteins. The total proteins were then probed by specific antibodies or IgG for 2 h at 4°C. Subsequently, the beads were mixed with the proteins and rotated overnight at 4°C. The immunoprecipitated complexes were collected by centrifugation, boiled for 5 min in sodium dodecyl sulfate loading buffer, and finally visualized by Western blot.

Western blot

The whole lysates of tissues and cells were obtained by incubating with RIPA lysis buffer according to the product instructions. The entire lysates were then centrifuged to accumulate the supernatant, and the total protein content in the supernatant was determined by the BCA kit (Beyotime, Shanghai, China). The protein samples were subsequently loaded onto 10% sodium dodecyl sulphate-polyacrylamide gel electrophoresis (SDA-PAGE) for electrophoresis. The separated proteins were then transferred to polyvinylidene fluoride (PVDF) membranes and experienced blockage by 5% non-fat milk for 1 h. The PVDF membranes loading with proteins were probed by primary antibodies (1:1000) overnight at 4°C, following incubation with horseradish peroxidase-conjugated goat anti-rabbit secondary antibody (1:2000, ab6721, Abcam, Shanghai, China) for 2 h at room temperature. The primary antibodies were: anti-USP37 (ab229092, Abcam,

Shanghai, China), anti-CDK4 (ab137675, Abcam, Shanghai, China), anti-Cyclin D1 (ab226977, Abcam, Shanghai, China), anti-p21 (ab227443, Abcam, Shanghai, China), anti-Cleaved Caspase-3 (ab2302, Abcam, Shanghai, China), anti-total Caspase-3 (ab44976, Abcam, Shanghai, China), anti-MMP2 (ab97779, Abcam, Shanghai, China), anti-E-cadherin (ab15148, Abcam, Shanghai, China), anti-N-cadherin (ab18203, Abcam, Shanghai, China), anti-Snail (abs155342, Absin Biotechnology, Shanghai, China), anti-Vimentin (ab137321, Abcam, Shanghai, China), anti-ALDH1 (abs136145, Absin Biotechnology, Shanghai, China), anti-OCT4 (ab18976, Abcam, Shanghai, China), anti-β-catenin (ab16051, Abcam, Shanghai, China) and anti-β-actin (ab8227, Abcam, Shanghai, China). Following that, the ECL kit (Beyotime, Shanghai, China) was used to make particular protein blots. Image J software (NIH, Bethesda, MD, USA) executed the gray value detection of the protein blots. β-actin was set as the reference.

Statistical analysis

The experiments in this article were implemented in triplicates. Statistical analysis was carried out using SPSS 20.0 software, and the graphs were created using GraphPad Prism 6 software. All data were presented in the form of mean ± standard deviation. Paired Student's t-test was executed to analyze the difference between the two groups. One-way analysis of variance and Tukey's post hoc test were employed for the data comparison in more than two groups. $P < 0.05$ revealed a statistically significant difference.

Results

USP37 expression was abnormally increased in CRC patients

The primary goal of this study was to see if USP37 was dysregulated in CRC by evaluating data from the TCGA database. The results revealed that the level of USP37 in COAD tissues was significantly higher than that in nearby normal tissues ($P < 0.01$ and $P < 0.001$) (**Figure 1A**). The level of USP37 mRNA in clinical tissues of 106 CRC cases was detected next. As a result, tumor tissues had considerably greater levels of USP37 mRNA than nearby normal tissues ($P < 0.01$) (**Figure 1B**). The Kaplan-Meier survival curve was used to investigate the effect of the USP37 level on the survival of CRC cases. According to the findings, CRC patients with high USP37 level (n = 53) had poor 2000-day survival rate than those with low USP37 level (n = 53) ($P < 0.05$) (**Figure 1C**). IHC and Western blot of clinical samples showed higher USP37 protein level in tumor tissues than in neighboring normal tissues ($P < 0.01$) (**Figure 1D** and **1E**). Thus, it was discovered that USP37 was up-modulated in CRC patients.

USP37 intensified the proliferation and attenuated apoptosis of CRC cells

This study used Western blot to confirm the *in vitro* expression of USP37 protein. Compared to the normal human intestinal epithelial cell line (NCM460), CRC cell lines (HCT116, SW620, LoVo, SW480 and T84) had significantly higher USP37 protein expression ($P < 0.01$) (**Figure 2A**). HCT116 and T84 cell lines were used for this research, as they expressed higher USP37 protein than the other three CRC cell lines.

USP37 protein expression was regulated by separately transfecting USP37 vectors, empty vectors, shUSP37-#1, shUSP37-#2 and scramble into HCT116 and T84 cells. The USP37 group had higher USP37 protein levels in HCT116 and T84 cells than the Control group (**Figure 2B**). In contrast, lower USP37 protein level was observed in HCT116 and T84 cells of the shUSP37-1# and shUSP37-2# groups compared to the Scramble group ($P < 0.01$). Thereby, the expression of USP37 protein was effectively modulated by transfection.

The proliferation, cell cycle, and apoptosis of cells were then evaluated by MTT and flow cytometry assays. Matched to the Control group, HCT116 and T84 cells from the USP37 group showed increased proliferation, reduced proportion of cells in the G1 phase, increased proportion of cells in the S phase, and declined proportion of apoptosis ($P < 0.01$). In contrast to Scramble group, HCT116 and T84 cells of the shUSP37-1# and shUSP37-2# groups displayed restrained proliferation, elevated proportion of cells in the G1 phase, reduced proportion of cells in the S phase, and increased proportion of apoptosis ($P < 0.01$) (**Figure 2C-E**). As a result, USP37 intensified the prolif-

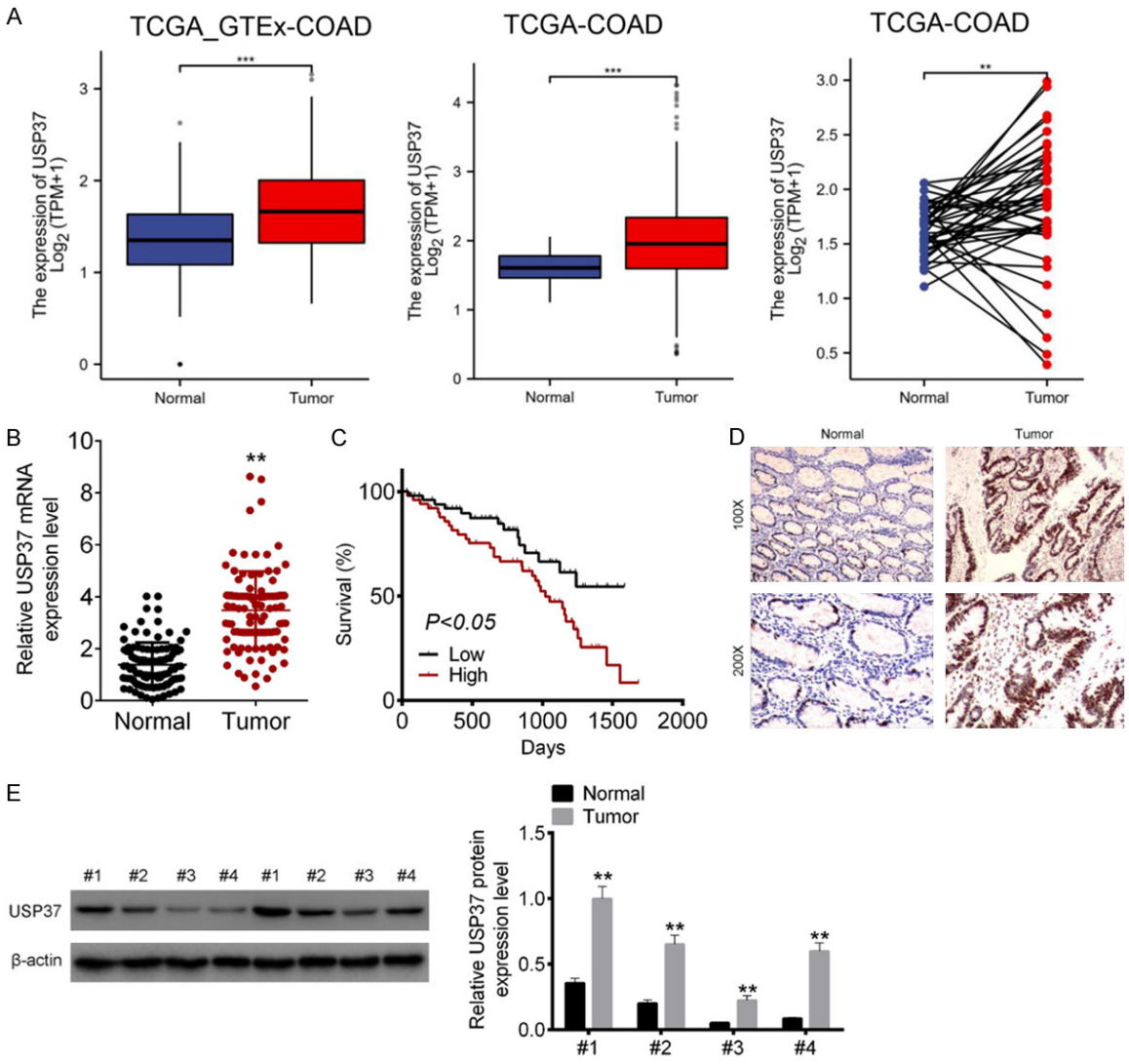

Figure 1. USP37 expression was abnormally increased in CRC patients. A. USP37 level in COAD patients was analyzed according to the data collected from TCGA database. B. USP37 level in tumor tissues as well as paired adjacent normal tissues of 106 CRC cases was evaluated by qRT-PCR. C. The effect of USP37 level on the survival of 106 CRC cases was explored by Kaplan-Meier survival curve. D. IHC of clinical samples to monitor the expression of USP37 protein. Magnification: 100 × or 200 ×. E. Western blot of clinical samples to explore the level of USP37 protein. $^{**}P < 0.01$ and $^{***}P < 0.001$.

eration, cell cycle progression, and attenuated apoptosis of CRC cells.

Western blot was used to investigate the effect of USP37 on the cell cycle- and apoptosis-related protein expression. Compared to the Control group, HCT116 and T84 cells from the USP37 group had higher CDK4 and Cyclin D1 protein levels but lower p21 and cleaved caspase-3/total Caspase-3 proteins levels ($P < 0.01$). However, the reduced CDK4 and Cyclin D1 proteins level, and the elevated p21 and Cleaved Caspase-3/total Caspase-3 proteins level, occurred in HCT116 and T84 cells of the shUSP37-1# and shUSP37-2# groups when compared to the Scramble group ($P < 0.01$) (**Figure 2F**). Thus, USP37 might intensify the proliferation, cell cycle progression, and attenuate apoptosis of CRC cells via regulating the cell cycle- and apoptosis-related protein expression.

USP37 exacerbated the migration, invasion, EMT and stemness capacities of CRC cells

This study performed wound healing and Transwell assays to examine the effect of USP37 on the migration and invasion capaci-

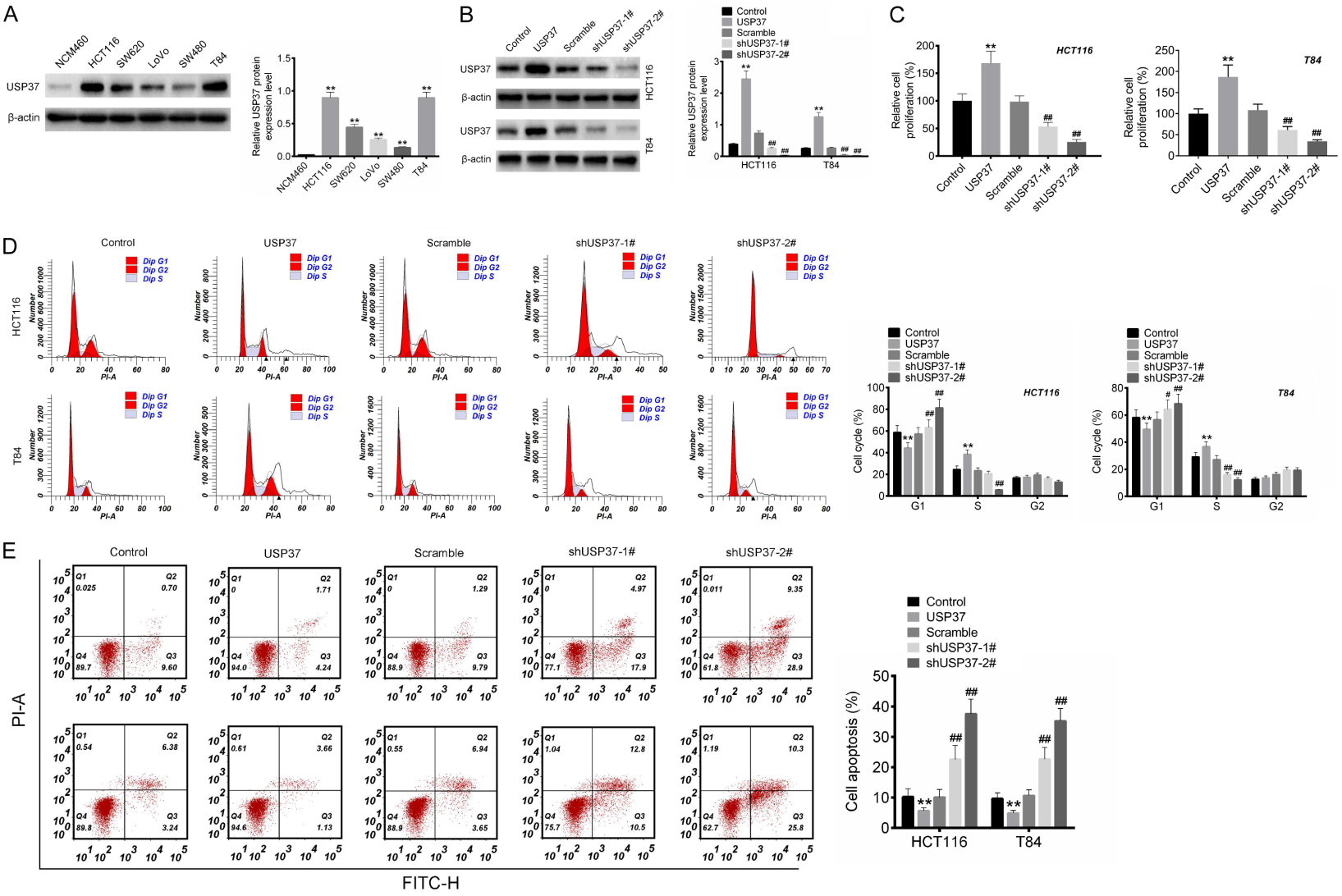
A
NCM460
HCT116
SW620
LoVo
SW480
T84
USP37
β-actin
Relative USP37 protein expression level
B
Control
USP37
Scramble
shUSP37-1#
shUSP37-2#
HCT116
T84
C
HCT116
T84
Relative cell proliferation (%)
D
Control
USP37
Scramble
shUSP37-1#
shUSP37-2#
Dip G1
Dip G2
Dip S
PI-A
Number
Cell cycle (%)
G1
S
G2
E
Q1
Q2
Q3
Q4
PI-A
FITC-H
Cell apoptosis (%)

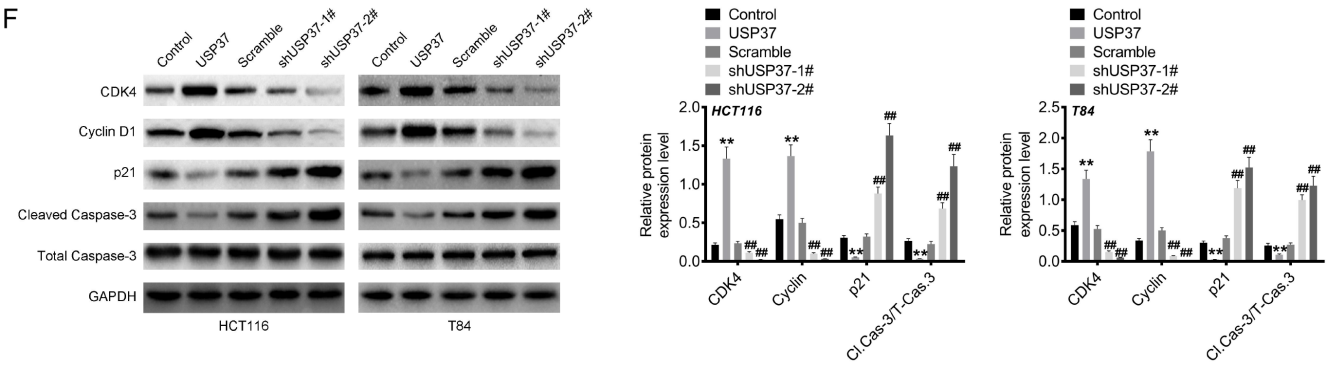

Figure 2. USP37 intensified the proliferation and attenuated apoptosis of CRC cells. A. USP37 protein expression in normal human intestinal epithelial cell line (NCM460) and CRC cell lines (HCT116, SW620, LoVo, SW480 and T84) was researched by Western blot. B. Western blot was implemented to verify the transfection efficiency of CRC cells. C. MTT assay was employed to detect the proliferation capacity of CRC cells. D and E. Flow cytometry assay was executed to monitor the cell cycle and apoptosis of CRC cells. F. Cell cycle- and apoptosis-related protein expression was assessed by Western blot. $^{**}P < 0.01$ vs. NCM460 cell line or Control group. $^{\#\#}P < 0.01$ vs. Scramble group.

ties of CRC cells. **Figure 3A** and **3B** show the reduced wound width and the increased invasion cell number in HCT116 and T84 cells of the USP37 group compared to the Control group ($P < 0.01$). In contrast to the Scramble group, higher relative wound width and lower invasion cell number was found in HCT116 and T84 cells of the shUSP37-1# and shUSP37-2# groups ($P < 0.01$). Sphere-forming assay was utilized to evaluate the effect of USP37 on the stemness of CRC cells. As a result, HCT116 and T84 cells of USP37 group could form more spheres than those of Control group. Conversely, the reduced spheres were observed in HCT116 and T84 cells of shUSP37-1# and shUSP37-2# groups, in comparison to Scramble group (**Figure 3C**). Western blot was used to assess the expression of EMT- and stemness-related proteins. Compared to the Control group, the USP37 group had higher levels of MMP2, N-cadherin, Snail, Vimentin, ALDH1 and OCT4 proteins, but lower level of E-cadherin protein in HCT116 and T84 cells ($P < 0.01$). When compared to the Scramble group, the shUSP37-1# and shUSP37-2# groups had lower levels of MMP2, N-cadherin, Snail, Vimentin, ALDH1 and OCT4 proteins, but higher level of E-cadherin protein was observed in HCT116 and T84 cells ($P < 0.01$) (**Figure 3D**). Therefore, USP37 intensified the migration, invasion, EMT and stemness abilities of CRC cells.

USP37 promoted the angiogenic ability of HUVECs

The culture media of transfected HCT116 and T84 cells was collected to culture HUVECs to investigate their migratory abilities using the Transwell assay. Higher migration cell number was observed in HUVECs of the USP37 group in contrast to the Control group ($P < 0.01$). However, the migration cell number declined in HUVECs of the shUSP37-1# and shUSP37-2# groups when compared with the Scramble group ($P < 0.01$) (**Figure 4A**). Furthermore, in the angiogenesis assay, a higher tube number was monitored in HUVECs of the USP37 group compared to the Control group ($P < 0.01$). HUVECs of the shUSP37-1# and shUSP37-2# groups had fewer tubes than the Scramble group ($P < 0.01$) (**Figure 4B**). ELISA was used to measure the level of VEGFA in the culture medium of HUVECs. Compared to the Control group, the VEGFA level was elevated in the culture medium of HUVECs in the USP37 group ($P < 0.01$). In contrast, a lower VEGFA level was observed in the culture medium of HUVECs cells in the shUSP37-1# and shUSP37-2# groups when compared to the Scramble group ($P < 0.01$) (**Figure 4C**). These findings suggested that USP37 promoted the angiogenic ability of HUVECs.

USP37 silencing attenuated the in vivo growth and lung metastasis of CRC

This study established a xenograft model by subcutaneously injecting HCT116 cells into nude mice to investigate the effect of USP37 on CRC *in vivo* growth. In comparison to mice injected with scramble-treated HCT116 cells, mice injected with shUSP37-treated HCT116 cells showed lower tumor volume and weight ($P < 0.05$ and $P < 0.01$) (**Figure 5A**). The xenograft tumor tissues collected from mice injected with shUSP37-treated HCT116 cells showed less Ki67 protein expression than those collected from mice injected with scramble-treated HCT116 cells (**Figure 5B**).

This study injected HCT116 cells into nude mice through the tail vein to investigate the effect of USP37 on CRC *in vivo* lung metastasis. The lung tissues were harvested for HE staining. Lung tissues of mice injected with shUSP37-treated HCT116 cells exhibited fewer nodules than those injected with scramble-treated HCT116 cells (**Figure 5C**). These findings suggested that USP37 silencing attenuated the *in vivo* growth and lung metastasis of CRC.

USP37 expression was positively correlated with β-catenin in CRC

β-catenin is coded by CTNNB1, which has been identified as an oncogene in CRC. Using the TCGA-COAD and TCGA-READ datasets, this study investigated the correlation between USP37 and CTNNB1. The results showed a positive correlation between USP37 and CTNNB1 ($P < 0.001$) (**Figure 6A**). To further verify the relationship between USP37 and β-catenin, the study detected the expression of USP37 and β-catenin in clinical tissues of CRC cases by IHC. As a result, β-catenin was highly expressed in CRC tissues. Meanwhile, in USP37 high expression clinical CRC tissues, a high level of β-catenin was also found. Accordingly, a low β-catenin level was observed in USP37 low

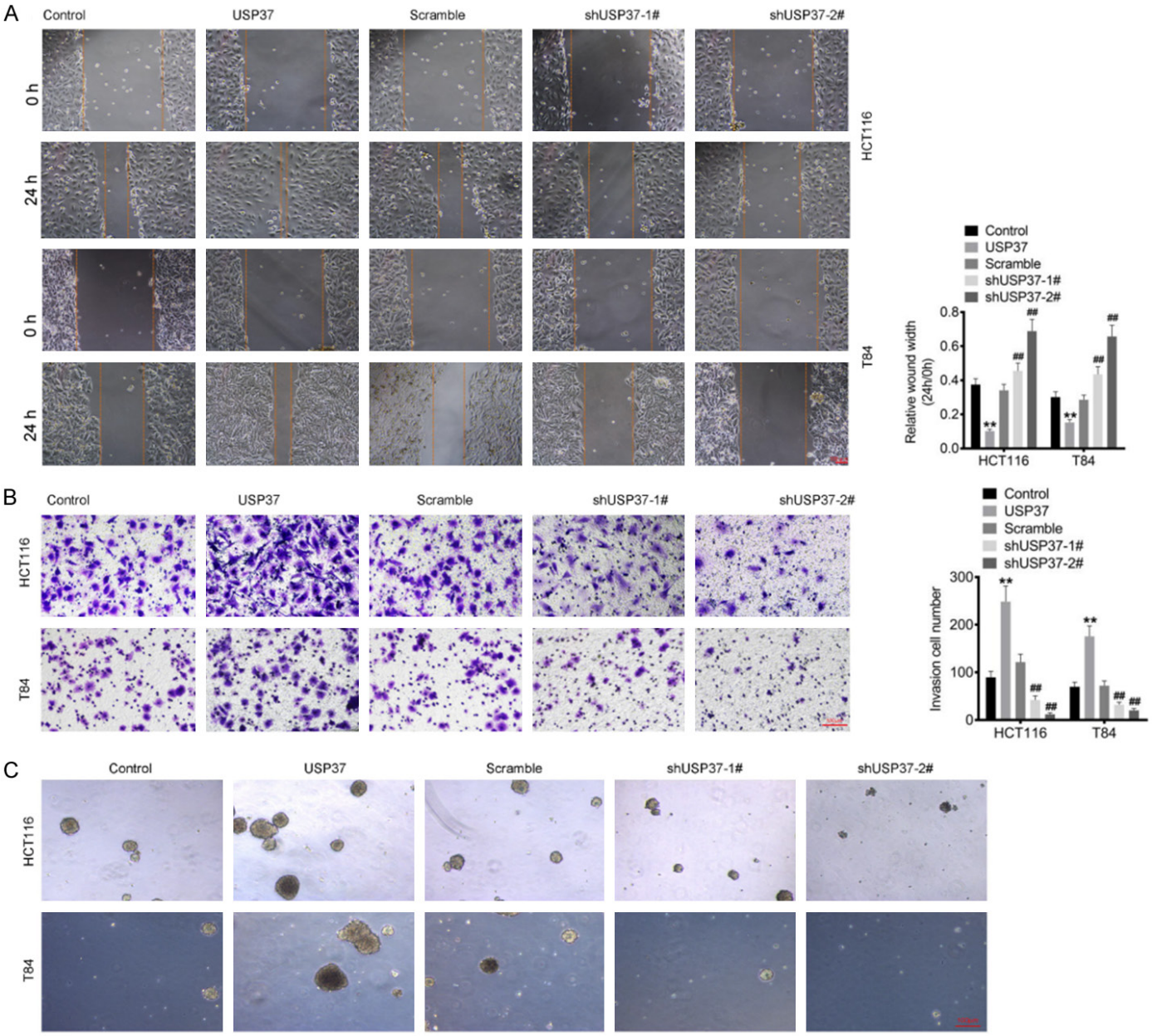
A
Control
USP37
Scramble
shUSP37-1#
shUSP37-2#
0 h
24 h
0 h
24 h
HCT116
T84
Control
USP37
Scramble
shUSP37-1#
shUSP37-2#
Relative wound width (24h/0h)
0.8
0.6
0.4
0.2
0.0
HCT116
T84
B
Control
USP37
Scramble
shUSP37-1#
shUSP37-2#
HCT116
T84
Control
USP37
Scramble
shUSP37-1#
shUSP37-2#
Invasion cell number
300
200
100
0
HCT116
T84
C
Control
USP37
Scramble
shUSP37-1#
shUSP37-2#
HCT116
T84

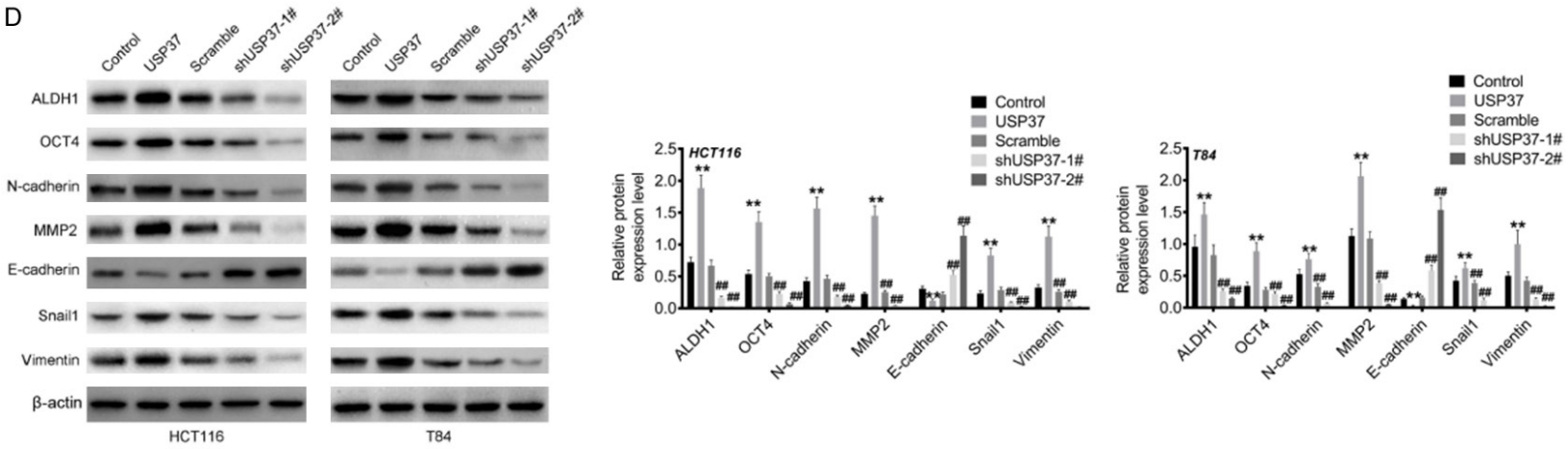

Figure 3. USP37 exacerbated the migration and invasion capacities of CRC cells. A. Wound healing assay was recruited to assess the migration capacity of CRC cells. Magnification: 200 ×. B. Transwell assay was executed to evaluate the invasion ability of CRC cells. Magnification: 200 ×. C. Sphere-forming assay was utilized to evaluate the stemness of CRC cells. Magnification: 200 ×. D. The expression of EMT- and stemness-related proteins was detected by Western blot. $^{**}P < 0.01$ vs. Control group. $^{\#\#}P < 0.01$ vs. Scramble group.

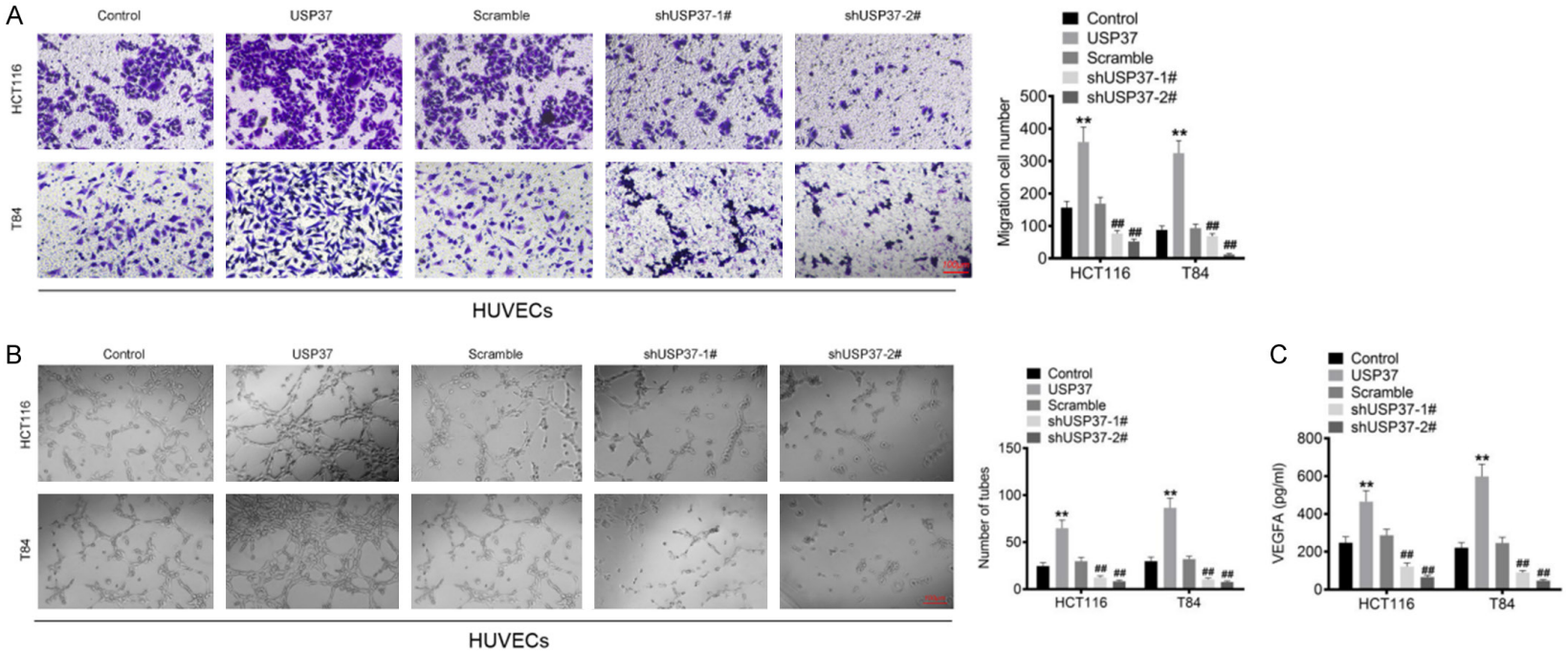

Figure 4. USP37 promoted the angiogenic ability of HUVECs. A. The culture medium of the transfected HCT116 and T84 cells was collected to culture HUVECs, and then the migration ability of HUVECs was evaluated by Transwell assay. Magnification: 200 ×. B. The culture medium of the transfected HCT116 and T84 cells was collected to culture HUVECs. Then angiogenesis assay was employed to explore the angiogenic ability of HUVECs. Magnification: 200 ×. C. The culture medium of the transfected HCT116 and T84 cells was collected to culture HUVECs. Then the VEGFA level in the culture medium of HUVECs cells was detected by ELISA. $^{**}P < 0.01$ vs. Control group. $^{\#\#}P < 0.01$ vs. Scramble group.

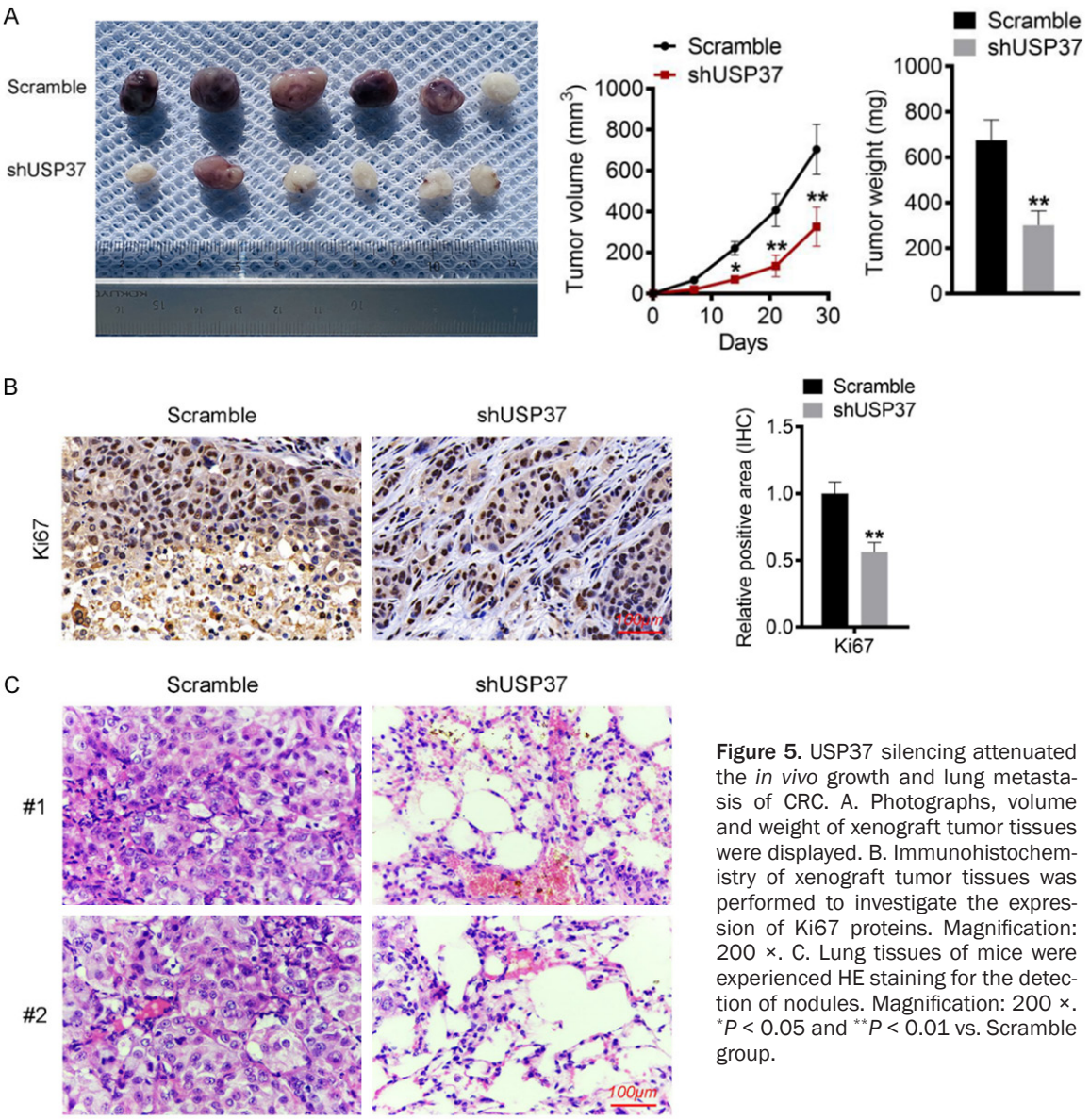

Figure 5. USP37 silencing attenuated the *in vivo* growth and lung metastasis of CRC. A. Photographs, volume and weight of xenograft tumor tissues were displayed. B. Immunohistochemistry of xenograft tumor tissues was performed to investigate the expression of Ki67 proteins. Magnification: 200 ×. C. Lung tissues of mice were experienced HE staining for the detection of nodules. Magnification: 200 ×. $^{*}P < 0.05$ and $^{**}P < 0.01$ vs. Scramble group.

expression clinical CRC tissues (**Figure 6B**). This study also used IHC to monitor the expression of USP37 and β-catenin in xenograft tumor tissues. In comparison to xenograft tumor tissues collected from mice injected with scramble-treated HCT116 cells, those collected from mice injected with shUSP37-treated HCT116 cells displayed lower USP37 and β-catenin expression ($P < 0.01$) (**Figure 6C**). Thus, USP37 expression was positively correlated with β-catenin in CRC.

USP37 could intensify the stability of β-catenin by inhibiting its ubiquitination

The role of USP37 on the expression of β-catenin was investigated by Western blot. Compared to the Control group, the HCT116 and T84 cells of the USP37 group had higher levels of both USP37 and β-catenin proteins ($P < 0.01$). Simultaneously, in contrast to the Scramble group, the level of USP37 and β-catenin proteins were decreased in HCT116 and T84 cells of the shUSP37-1# and shUSP37-2# groups ($P < 0.01$) (**Figure 7A**). Thus, USP37 could facilitate the expression of β-catenin in CRC cells.

The mechanism of USP37 in regulating β-catenin expression by co-immunoprecipitation was further verified using 293T cells. When USP37 and β-catenin were co-precipitated, they were co-expressed, indicating an interaction between USP37 and β-catenin (**Figure 7B**).

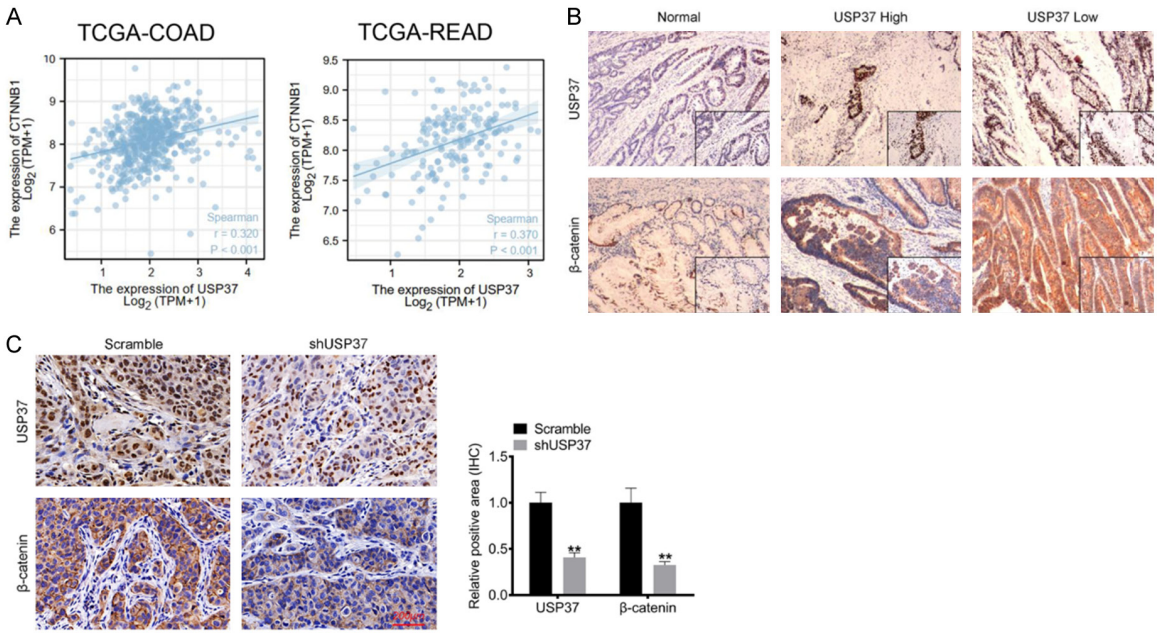

Figure 6. USP37 expression was positively correlated with β-catenin in CRC. A. The correlation between USP37 and CTNNB1 (coding β-catenin protein) in CRC cases was analyzed based on the TCGA-COAD and TCGA-READ databases. B. USP37 and β-catenin expression in clinical CRC tissues was monitored by immunohistochemical. Magnification: 200 ×. C. USP37 and β-catenin expression detection in xenograft tumor tissues was executed by immunohistochemical. Magnification: 200 ×. $^{**}P < 0.01$ vs. Scramble group.

As a result, MG132 was used to treat the HCT116 and T84 cells to investigate the mechanism by which USP37 regulates β-catenin expression. Both USP37 overexpression and MG132 treatment were observed to increase the level of β-catenin in HCT116 and T84 cells. However, USP37 silencing could reduce the expression of β-catenin in HCT116 and T84 cells. Intriguingly, MG132 treatment could reverse the inhibition of USP37 silencing on β-catenin expression in HCT116 and T84 cells (**Figure 7C**). These results suggested that USP37 increased the β-catenin protein level via the proteasome-dependent pathway. Subsequently, we used CHX to treat HCT116 and T84 cells to explore whether USP37 increased β-catenin protein level via inhibiting its degradation. In the presence of CHX, USP37 silencing accelerated the degradation of β-catenin, but USP37 overexpression delayed β-catenin degradation (**Figure 7D**). Further, the influence of USP37 on the ubiquitination of β-catenin protein was explored. As shown in Figure S1, USP37 silencing obviously promoted the ubiquitination level of β-catenin protein. Thus, it was demonstrated that USP37 increased the level of β-catenin in CRC by intensifying its stability via inhibiting its ubiquitination.

Discussion

Currently, there is no direct evidence to uncover the exact function and carcinogenic mechanism of USP37 in CRC. Firstly, the oncogenicity of USP37 in the progression of CRC was investigated. The findings suggested that USP37 was abnormally overexpressed in CRC patients and that high USP37 expression was associated with poor patient outcome. *In vitro* study revealed that USP37 intensified the proliferation, cell cycle progression, apoptosis inhibition, migration and invasion of CRC cells and angiogenic ability of HUVECs. According to *in vivo* study, USP37 silencing inhibited the growth and lung metastasis of CRC in nude mice. Regarding the internal mechanism, USP37 accelerated the stability of β-catenin protein by suppressing its ubiquitination to enhance the progression of CRC. USP37 has been found to have oncogenic activity in several human cancers, including breast cancer, gastric cancer, kidney cancer and lung cancer [14-17]. This study established the oncogenic activity of USP37 in CRC for the first time.

This study indicated that USP37 up-regulation intensified the expression of CDK4 and Cyclin

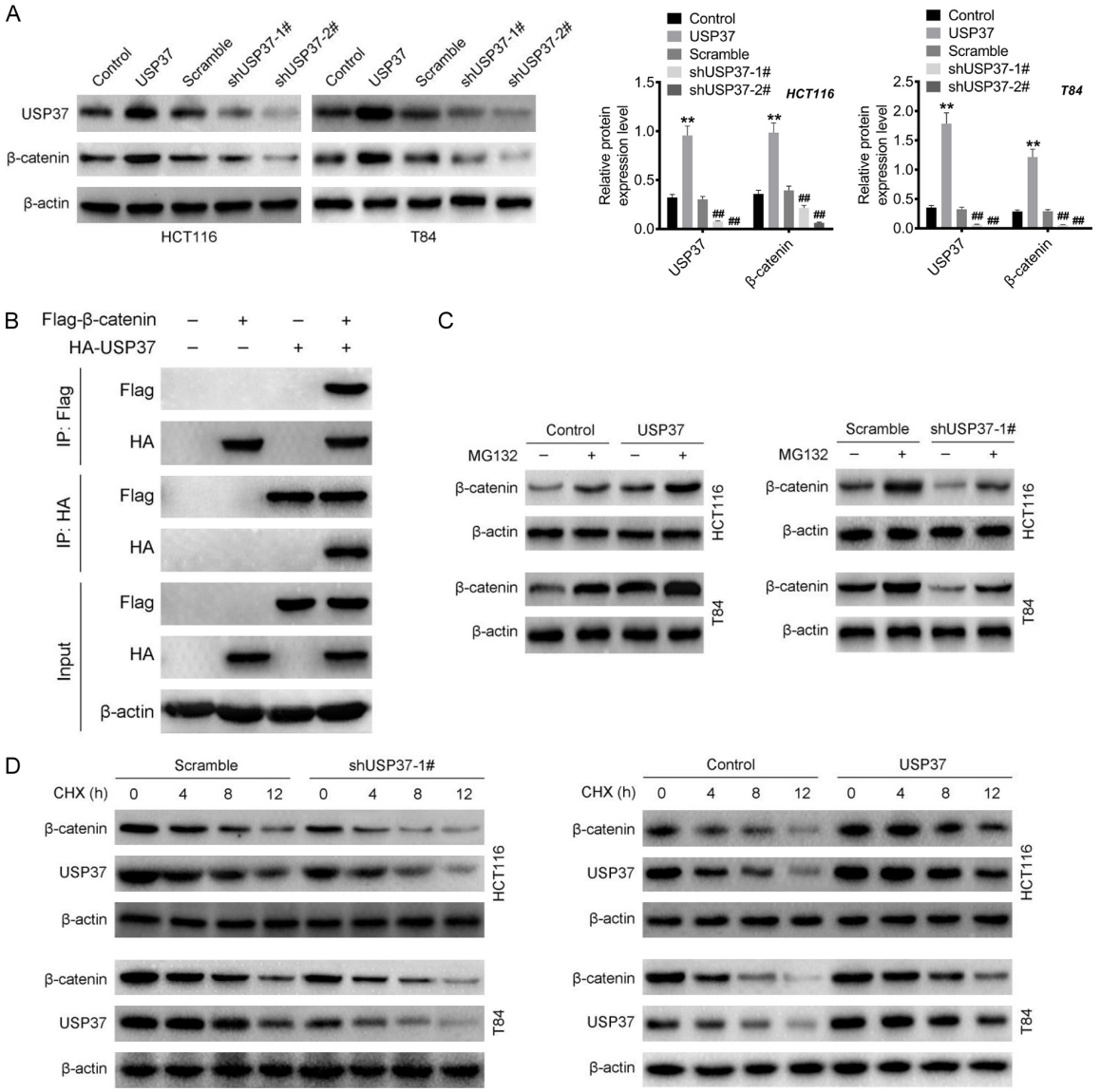

Figure 7. USP37 could intensify the stability of β-catenin. A. The function of USP37 on the expression of β-catenin in CRC cells was investigated by Western blot. $^{**}P < 0.01$ vs. Control group. $^{\#\#}P < 0.01$ vs. Scramble group. B. Co-immunoprecipitation was performed on 293T cells to verify the interaction between USP37 and β-catenin. C and D. MG132 and CHX treatment was implemented on CRC cells to verify the mechanism of USP37 in regulating β-catenin expression.

D1 proteins while decreasing the expression of p21 and Cleaved Caspase-3 proteins in CRC cells. CDK4 dysregulation is common in cancer, and can facilitate the transition of the cell cycle from the G1 phase to the S phase, which can therefore accelerate cell cycle progression as well as tumor cell proliferation and growth [20]. Similarly, in cancers, the over-activated Cyclin D1 accelerates cell cycle progression, resulting in the uncontrolled proliferation of tumor cells [21]. p21 has been shown to possess anti-tumor activity, as indicated by its inhibitory role in the proliferation and growth of tumor cells, as well as its role in maintaining G1 cell cycle arrest [22]. According to the findings, USP37 might facilitate the cell cycle progression and proliferation of CRC cells by intensifying the expression of Cyclin D1 and CDK4 proteins while decreasing the expression of p21 proteins. The apoptosis of tumor cells is generally acknowledged as one of the leading factors influencing the progression of tumors. Cleaved Caspase-3 is a critical apoptosis-related protein that acts as one of the primary cardinal

executioners, activating its downstream effectors to facilitate the apoptosis of cells [23]. As a result, USP37 was shown to inhibit the apoptosis of CRC cells by suppressing the expression of the Cleaved Caspase-3 protein. A previous study found that USP37 silencing increased the expression of the Cleaved Caspase-3 protein, which induced the apoptosis of breast cancer cells [12]. This study discovered similar findings in CRC.

It has been revealed that USP37 has a role in EMT promotion in human tumor cells [15]. Interestingly, this article revealed the promotion role of USP37 in EMT in CRC, as USP37 enhanced the expression of MMP2, N-cadherin, Snail, Vimentin proteins but reduced the expression of E-cadherin protein. EMT plays a key role in the metastasis of tumors. The primary characteristic of EMT is the loss of tight connections between cells, which allows cells to become more invasive [24]. Degradation of extracellular matrix proteins by MMP2 is the first step enabling tumor cells to invade more frequently [25]. During EMT, the expression of E-cadherin protein, a major EMT symbol, is diminished [26]. N-cadherin, Snail and Vimentin serve a central role in activating EMT, because they are able to disrupt the basement membrane and cause epithelial cells to detach from each other [27, 28]. In this paper, USP37 could intensify the EMT in CRC cells by regulating these EMT-associated proteins. Moreover, USP37 silencing restrained the *in vivo* growth and lung metastasis of CRC. Thus, it might be that USP37 facilitated the metastasis in CRC by enhancing the EMT. Additionally, this study suggested that USP37 promoted the stemness of CRC cells and expression of ALDH1 and OCT4 proteins in CRC cells. The stemness has been confirmed to promote the tumourigenicity, drug-resistance, relapse and metastasis of tumors, which is considered to be a “root” of aggressive tumors [24]. ALDH1 is a useful biomarker for the identification of stemness and OCT4 is proved to be a critical promoter of stemness [29, 30]. In this paper, USP37 was suggested to enhance the stemness of CRC cells.

Angiogenesis is a known and critical indicator for evaluating the degree of tumor malignancy. Tumor cells can sustain their oxygen and nutrient supply by promoting angiogenesis [31]. Angiogenesis has emerged as a therapy focus for CRC, particularly for metastatic CRC [32]. VEGFA is an essential regulator of angiogenesis, and some VEGFA inhibitor (such as bevacizumab) has been approved to be the first-line treatment drug for CRC by the Food and Drug Administration (FDA) [33]. In this study, USP37 has been proven to facilitate the *in vitro* angiogenic ability and intensify the secretion of VEGFA in HUVECs. These discoveries provided essential theoretical basis for targeting USP37 in CRC treatment.

Importantly, this study demonstrated that USP37 expression was associated with β-catenin expression in CRC. USP37 silencing reduced β-catenin expression in xenograft tumor tissues. USP37 might enhance the stability of the β-catenin protein in CRC cells. β-catenin protein has been found to accumulate in multiple types of cancer cells, where it can translocate into the nucleus to exert oncogenic activity (such as promoting EMT) by binding to the T cell factor/lymphoid enhancer factor (TCF/LEF) family of transcription factors [18, 34]. Additionally, in the absence of TCF/LEF, β-catenin can regulate the expression of β-catenin-dependent genes, promoting tumor malignancy [35]. β-catenin is a crucial regulator of normal intestinal stem cell homeostasis, controlling the differentiation of normal intestinal stem cells into distinct cell types. In CRC, however, β-catenin is abnormally activated. It is an important marker of poor prognosis in CRC patients and is crucial for the self-renewal of CRC stem cells [36, 37]. This study suggested that USP37 may facilitate the progression of CRC by increasing the stability of the β-catenin protein. As a deubiquitinating enzyme, an important mechanism for the pro-tumor progression of USP37 is through the inhibition of ubiquitination of multiple proteins [38, 39]. It has been reported that USP37 can enhance the progression of gastric cancer and lung cancer by deubiquitination of Snail [16, 17]. Similarly, this study revealed that USP37 silencing promoted the ubiquitination level of β-catenin protein in CRC cells. Thus, USP37 might intensify the stability of β-catenin protein by inhibiting its ubiquitination, thereby facilitating the progression of CRC.

Conclusion

This study explored the carcinogenic activity of USP37 in CRC. Patients with CRC with high USP37 expression had a poor chance of sur-

vival. USP37 could intensify the *in vitro* proliferation, migration, invasion, EMT, and stemness of CRC cells, and the angiogenic ability of HUVECs. Moreover, the silencing of USP37 restricted the *in vivo* growth and lung metastasis of CRC in nude mice. Mechanically, USP37 accelerated the stability of β-catenin protein via inhibiting its ubiquitination, thereby enhancing the progression of CRC. USP37 might be a suitable target for CRC treatment. It might be a promising strategy to treat CRC with drugs possessing the USP37-inhibition effect.

Disclosure of conflict of interest

None.

Address correspondence to: Drs. Enda Yu and Jifu E, Department of Colorectal Surgery, Changhai Hospital, Navy Military Medical University, No. 168 Changhai Road, Shanghai 200433, China. Tel: +86-021-31161612; E-mail: wzm287964403@126.com (EDY); changhaiejf@163.com (JFE)

References

[1] Ibrahiem AT, Fawzy MS, Abu AlSel BT and Toraih EA. Prognostic value of BRAF/MIR-17 signature and B-Raf protein expression in patients with colorectal cancer: a pilot study. J Clin Lab Anal 2021; 35: e23679.

[2] Ji G, Zhou W, Li X, Du J, Li X and Hao H. Melatonin inhibits proliferation and viability and promotes apoptosis in colorectal cancer cells via upregulation of the microRNA-34a/449a cluster. Mol Med Rep 2021; 23: 187.

[3] Chang N, Cui Y, Liang X, Han D, Zheng X, Wu A and Qian L. Long noncoding RNA LINC00857 promotes proliferation, migration, and invasion of colorectal cancer cell through miR-1306/vimentin axis. Comput Math Methods Med 2021; 2021: 5525763.

[4] Si H, Yang Q, Hu H, Ding C, Wang H and Lin X. Colorectal cancer occurrence and treatment based on changes in intestinal flora. Semin Cancer Biol 2021; 70: 3-10.

[5] Miller KD, Nogueira L, Mariotto AB, Rowland JH, Yabroff KR, Alfano CM, Jemal A, Kramer JL and Siegel RL. Cancer treatment and survivorship statistics, 2019. CA Cancer J Clin 2019; 69: 363-385.

[6] Zhou L, Chen Q, Wu J, Yang J, Yin H, Tian J, Gong L, Kong D and Tao M. miR-942-5p inhibits proliferation, metastasis, and epithelial-mesenchymal transition in colorectal cancer by targeting CCBE1. Biomed Res Int 2021; 2021: 9951405.

[7] Fu D, Chen Y and Xu D. Circulating miR-449a predicts survival outcome for colorectal cancer following curative resection: an observational study. Medicine (Baltimore) 2021; 100: e25022.

[8] Zhang QX, Wang XC, Chen SP and Qin XT. Predictive value of deubiquitination enzymes USP37 in the prognosis of breast cancer. Zhonghua Yi Xue Za Zhi 2016; 96: 944-948.

[9] Tanno H, Shigematsu T, Nishikawa S, Hayakawa A, Denda K, Tanaka T and Komada M. Ubiquitin-interacting motifs confer full catalytic activity, but not ubiquitin chain substrate specificity, to deubiquitinating enzyme USP37. J Biol Chem 2014; 289: 2415-2423.

[10] Huang X, Summers MK, Pham V, Lill JR, Liu J, Lee G, Kirkpatrick DS, Jackson PK, Fang G and Dixit VM. Deubiquitinase USP37 is activated by CDK2 to antagonize APC(CDH1) and promote S phase entry. Mol Cell 2011; 42: 511-523.

[11] Burrows AC, Prokop J and Summers MK. Skp1-Cul1-F-box ubiquitin ligase (SCF(βTrCP))-mediated destruction of the ubiquitin-specific protease USP37 during G2-phase promotes mitotic entry. J Biol Chem 2012; 287: 39021-39029.

[12] Qin T, Cui XY, Xiu H, Huang C, Sun ZN, Xu XM, Li LH and Yue L. USP37 downregulation elevates the chemical sensitivity of human breast cancer cells to adriamycin. Int J Med Sci 2021; 18: 325-334.

[13] Kim MS, Kim SH, Yang SH and Kim MS. miR-4487 enhances gefitinib-mediated ubiquitination and autophagic degradation of EGFR in non-small cell lung cancer cells by targeting USP37. Cancer Res Treat 2022; 54: 445-457.

[14] Hong K, Hu L, Liu X, Simon JM, Ptacek TS, Zheng X, Liao C, Baldwin AS and Zhang Q. USP37 promotes deubiquitination of HIF2α in kidney cancer. Proc Natl Acad Sci U S A 2020; 117: 13023-13032.

[15] Qin T, Li B, Feng X, Fan S, Liu L, Liu D, Mao J, Lu Y, Yang J, Yu X, Zhang Q, Zhang J, Song B, Li M and Li L. Abnormally elevated USP37 expression in breast cancer stem cells regulates stemness, epithelial-mesenchymal transition and cisplatin sensitivity. J Exp Clin Cancer Res 2018; 37: 287.

[16] Wu L, Zhao N, Zhou Z, Chen J, Han S, Zhang X, Bao H, Yuan W and Shu X. PLAGL2 promotes the proliferation and migration of gastric cancer cells via USP37-mediated deubiquitination of Snail1. Theranostics 2021; 11: 700-714.

[17] Cai J, Li M, Wang X, Li L, Li Q, Hou Z, Jia H and Liu S. USP37 promotes lung cancer cell migration by stabilizing snail protein via deubiquitination. Front Genet 2020; 10: 1324.

[18] Li Q, Lai Q, He C, Fang Y, Yan Q, Zhang Y, Wang X, Gu C, Wang Y, Ye L, Han L, Lin X, Chen J, Cai

J, Li A and Liu S. RUNX1 promotes tumour metastasis by activating the Wnt/β-catenin signalling pathway and EMT in colorectal cancer. J Exp Clin Cancer Res 2019; 38: 334.
[19] He Z, Dang J, Song A, Cui X, Ma Z and Zhang Y. The involvement of miR-150/β-catenin axis in colorectal cancer progression. Biomed Pharmacother 2020; 121: 109495.
[20] Hamilton E and Infante JR. Targeting CDK4/6 in patients with cancer. Cancer Treat Rev 2016; 45: 129-138.
[21] Montalto FI and De Amicis F. Cyclin D1 in cancer: a molecular connection for cell cycle control, adhesion and invasion in tumor and stroma. Cells 2020; 9: 2648.
[22] Liu L, Peng C, Ruan Y and Zhang Q. The natural product lapiferin inhibits cell proliferation and promotes cell apoptosis in gingival squamous cell carcinoma via P21 regulation. Mol Med Rep 2021; 24: 482.
[23] Zou J, Zhang Y, Sun J, Wang X, Tu H, Geng S, Liu R, Chen Y and Bi Z. Deoxyelephantopin induces reactive oxygen species-mediated apoptosis and autophagy in human osteosarcoma cells. Cell Physiol Biochem 2017; 42: 1812-1821.
[24] Tang Q, Chen J, Di Z, Yuan W, Zhou Z, Liu Z, Han S, Liu Y, Ying G, Shu X and Di M. TM4SF1 promotes EMT and cancer stemness via the Wnt/β-catenin/SOX2 pathway in colorectal cancer. J Exp Clin Cancer Res 2020; 39: 232.
[25] Xu H, Dun S, Gao Y, Ming J, Hui L and Qiu X. TMEM107 inhibits EMT and invasion of NSCLC through regulating the Hedgehog pathway. Thorac Cancer 2021; 12: 79-89.
[26] Mahmood MQ, Ward C, Muller HK, Sohal SS and Walters EH. Epithelial mesenchymal transition (EMT) and non-small cell lung cancer (NSCLC): a mutual association with airway disease. Med Oncol 2017; 34: 45.
[27] Tian X, Cao Z, Ding Q, Li Z and Zhang C. Prognostic value of multiple epithelial mesenchymal transition-associated proteins in intrahepatic cholangiocarcinoma. Oncol Lett 2019; 18: 2059-2065.
[28] Yao T, Hu W, Chen J, Shen L, Yu Y, Tang Z, Zang G, Zhang Y and Chen X. Collagen XV mediated the epithelial-mesenchymal transition to inhibit hepatocellular carcinoma metastasis. J Gastrointest Oncol 2022; 13: 2472-2484.
[29] Seino S, Shigeishi H, Hashikata M, Higashikawa K, Tobiume K, Uetsuki R, Ishida Y, Sasaki K, Naruse T, Rahman MZ, Ono S, Simasue H, Ohta K, Sugiyama M and Takechi M. CD44(high)/ALDH1(high) head and neck squamous cell carcinoma cells exhibit mesenchymal characteristics and GSK3β-dependent cancer stem cell properties. J Oral Pathol Med 2016; 45: 180-188.
[30] Dai Y, Yu T, Yu C, Lu T, Zhou L, Cheng C and Ni H. ISG15 enhances glioma cell stemness by promoting Oct4 protein stability. Environ Toxicol 2022; 37: 2133-2142.
[31] Lugano R, Ramachandran M and Dimberg A. Tumor angiogenesis: causes, consequences, challenges and opportunities. Cell Mol Life Sci 2020; 77: 1745-1770.
[32] Luo W, He D, Zhang J, Ma Z, Chen K, Lv Z, Fan C, Yang L, Li Y and Zhou Z. Knockdown of PPARδ induces VEGFA-mediated angiogenesis via interaction with ERO1A in human colorectal cancer. Front Oncol 2021; 11: 713892.
[33] Ferrara N and Adamis AP. Ten years of anti-vascular endothelial growth factor therapy. Nat Rev Drug Discov 2016; 15: 385-403.
[34] Bian J, Dannappel M, Wan C and Firestein R. Transcriptional regulation of Wnt/β-catenin pathway in colorectal cancer. Cells 2020; 9: 2125.
[35] Doumpas N, Lampart F, Robinson MD, Lentini A, Nestor CE, Cantù C and Basler K. TCF/LEF dependent and independent transcriptional regulation of Wnt/β-catenin target genes. EMBO J 2019; 38: e98873.
[36] Cho YH, Ro EJ, Yoon JS, Mizutani T, Kang DW, Park JC, Il Kim T, Clevers H and Choi KY. 5-FU promotes stemness of colorectal cancer via p53-mediated WNT/β-catenin pathway activation. Nat Commun 2020; 11: 5321.
[37] Wang Z, Zhou L, Xiong Y, Yu S, Li H, Fan J, Li F, Su Z, Song J, Sun Q, Liu SS, Xia Y, Zhao L, Li S, Guo F, Huang P, Carson DA and Lu D. Salinomycin exerts anti-colorectal cancer activity by targeting the β-catenin/T-cell factor complex. Br J Pharmacol 2019; 176: 3390-3406.
[38] Xiao Z, Chang L, Kim J, Zhang P, Hang Q, Yap S, Guo Y, Zhou Z, Zeng L, Hu X, Siverly A, Sun Y and Ma L. USP37 is a SNAI1 deubiquitinase. Am J Cancer Res 2019; 9: 2749-2759.
[39] Hong K, Hu L, Liu X, Simon JM, Ptacek TS, Zheng X, Liao C, Baldwin AS and Zhang Q. USP37 promotes deubiquitination of HIF2α in kidney cancer. Proc Natl Acad Sci U S A 2020; 117: 13023-13032.

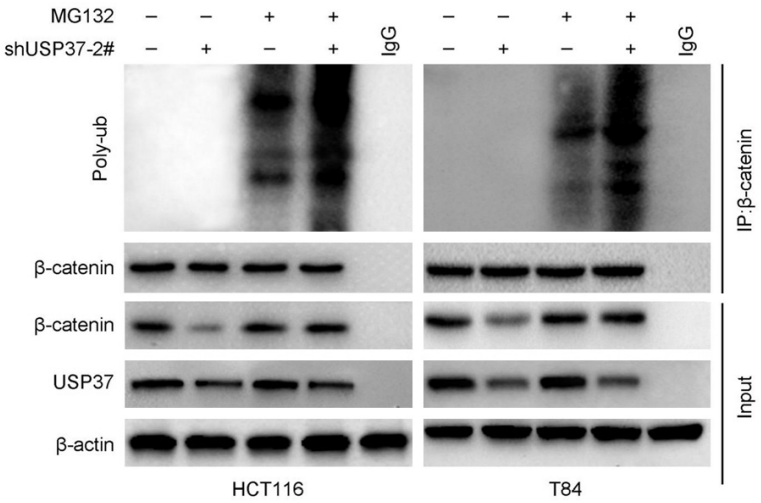

Figure S1. USP37 suppressed the ubiquitination level of β-catenin protein in CRC cells.